Science Advances
AAAS

advances.sciencemag.org/cgi/content/full/6/37/eabb1611/DC1

Supplementary Materials for

Dimorphism in cryptophytes—The case of *Teleaulax amphioxeia*/*Plagioselmis prolonga* and its ecological implications

A. Altenburger*, H. E. Blossom, L. Garcia-Cuetos, H. H. Jakobsen, J. Carstensen, N. Lundholm, P. J. Hansen, Ø. Moestrup, L. Haraguchi*

*Corresponding author. Email: andreas.altenburger@uit.no (A.A.); lumi.haraguchi@ymparisto.fi (L.H.)

Published 11 September 2020, *Sci. Adv.* **6**, eabb1611 (2020)
DOI: 10.1126/sciadv.abb1611

This PDF file includes:

Materials and Methods

DNA extraction, PCR and sequencing

DNA material: Cultures of *Teleaulax acuta* (SCCAP K-1486), *T. amphioxeia* (SCCAP K-1837) and *Geminigera cryophila* (RCC5152) were acquired and kept in f/2 or L1 growth medium at salinity 30 (f/2, 15°C for *Teleaulax* spp.; L1, 4 °C for *G. cryophila*). The Roskilde isolates were grown in L1 medium (salinity 12) with soil extract added (*41*) and kept at 10 °C. All cultures were kept with saturated light intensity (100 µmol photons $m^{-2}s^{-1}$), in a light/dark cycle of 16/8 h.
DNA extraction: Single cells were transferred to 0.2-mL PCR tubes containing 100 µl water and 10% (w/v) Chelex 100 (Sigma-Aldrich #C7901). For DNA extraction, the PCR tubes were vortexed for 5 s, spun down in a microcentrifuge for 10 s, and subsequently incubated at 95 ºC for 20 min (*42*). After incubation, the tubes were centrifuged again for 10 s and stored at 4 ºC until further use.
PCR: In the subsequent PCR reactions, 2 µL of the DNA extract was used as a template in a nested PCR approach. In the first PCR (25 µl reaction volume, 1.5 mM $MgCl_2$, 0.8 mM dNTPs [VWR #733-1363], 0.8 mg/mL BSA [BioLabs #B9000S], 0.5 units polymerase [VWR #733-1301], 0.8 µM primers SSUF and LSUR2), the full SSU, ITS, and part of the LSU rRNA were amplified. Nested PCRs were run using 0.5 µl from the first PCR as a template with the following primer sets: SSUF-SR7; SR4-SR9p; SR6-SSUR; ITS1-ITS4 (see Table S2). The mastermix was the same as above but without BSA. The following PCR conditions were used for the second PCR: 2 min at 95 ºC, followed by 25 cycles: 95 ºC for 30 s; 56 ºC for 30 s; 72 ºC for 50 s; followed by 5 min at 72 degrees. The presence of PCR products was confirmed on a 2 % agarose gel.
Sequencing: PCR products were sent to Macrogen (Macrogen Europe, Amsterdam, NL) for purification and sequencing in both directions. Sequence analysis (trimming, assembly, BLAST) was done with Geneious Prime version 2019.1.1 (Biomatters Ltd., Auckland, New Zealand). Accession numbers for the newly sequence strains are in Table 1.

Phylogenetic analyses

Cryptophyte sequences of 18S rDNA were downloaded from GenBank and aligned using MAFFT with subsequent alignment masking, as implemented in GUIDANCE2 (*43*, *44*). GUIDANCE alignment score was 0.983883, the masked alignment (columns below confidence score of 0.93 were removed) was trimmed by hand, included 1570 characters and was uploaded to the ATGC bioinformatics platform for PhyML 3.0 analysis with Smart Model Selection (the best model was TN93 +G+I), using the Akaike Information Criterion and performing 1000 bootstrap replicates (*45*, *46*). Bayesian Inference was performed with MrBayes 3.2.6 using a GTR+G+I model as implemented in Geneious Prime® 2019.1.1 (*47*). The following settings were used: four simultaneous Markov chain Monte Carlo (MCMC) run for 1,000,000 generations, sampling every 1000 generations. The first 25 % of trees were discarded as burn-in. Finally, a neighbour-joining tree was built, using the Jukes-Cantor genetic distance model and 10,000 bootstrap replicates as implemented in Geneious Prime version 2019.1.1.

Ploidy

Ploidy was determined from live material of *P. prolonga* and *T. amphioxeia* (Roskilde cultures). The cultures were checked for purity under the light microscope and by CytoSense before analysis. Due to the presence of stainable DNA materials other than the nuclei in the whole cells that would mask the ploidy signal, nuclei were isolated following a modified protocol from (*48*). Briefly, 15 mL of cultures in exponential growth phase were centrifuged (8944 g, 5 min.), the supernatant was removed, and the pellet was transferred to 2-mL Eppendorf tubes. The Eppendorf tubes were centrifuged (4930 g, 3 min), the supernatant was removed, and the pellet was resuspended in cold L1 media containing 0.1 % NP-40 (Sigma-Aldrich), and the ressuspension/ centrifugation step was repeated three times. The final pellet containing the isolated nuclei was resuspended in cold, pure L1 media, which was stored at 4°C until flow cytometric analysis (within 1 hour). The solution containing the isolated nuclei was stained for 10 min. with the nucleic acid stain SYBR green dye (1x final concentration) (*49*) and analyzed within 30 min. with CytoSense and CytoUSB, using a flow rate of 6 µL s^{-1} and a trigger of 100 mV for the FLY sensor. Nuclei were discriminated from other cell materials by a relative high FLY and low scattering, using the software CytoClus3 to determine the clusters manually. The ploidy level was determined using the intensity of FLY as a proxy for the amount of DNA in the nuclei. For cluster definitions, the extracted nuclei of the two cultures were analyzed first separately in order to define the cluster features for each individual culture. For nuclei comparison between the two cultures, the material of both cultures was mixed, processed and analyzed following the steps described above, in order to generate comparable histograms with both haploid and diploid nuclei in the same sample. Differences in the nuclei of each culture were described using the mean and standard deviation of the FLY peak and the total FLY.

Morphology

The general morphological features of cryptophytes, such as cell size and shape, furrow length and flagella (position and length), were investigated using an inverted light microscope (Nikon TI-U, Nikon Instruments Europe, NL) or an upright light microscope (Olympus BX53, Olympus Denmark, DK). Cell surface features were investigated in a scanning electron microscope JSM-6335F (Jeol, Japan). For fixation, 800 µL culture was added to a fixation cocktail of 960 µL 4 % aq. OsO_4, 960 µL growth medium and 480 µL saturated aq. $HgCl_2$, and left for 30 minutes. Samples were then collected in filters with a pore size of 2 µm, rinsed with Milli-Q water, and dehydrated in a graded ethanol series. They were critical-point dried and subsequently coated with Au-Pd before examination in the scanning electron microscope. In some cases, cells were fixed in acid Lugol solution, dehydrated in a graded ethanol series, critical point dried and coated with platinum.

CytoSense specifications

CytoSense is designed for the analysis of phytoplankton and allows for the identification of different groups based on their optical signatures, reflecting characteristics such as volume, shape, and pigment composition (*50, 51*). The CytoSense used in this study has a 488-nm laser, and a filter set adjusted for three fluorescence bands (FLR, em.: 650−700 nm for chlorophyll a; FLO, em.: 600-650 nm for phycoerythrin; and FLY, em.: 550 nm for FITC dyes) and sideward (SWS) and forward (FWS) scatter sensors.

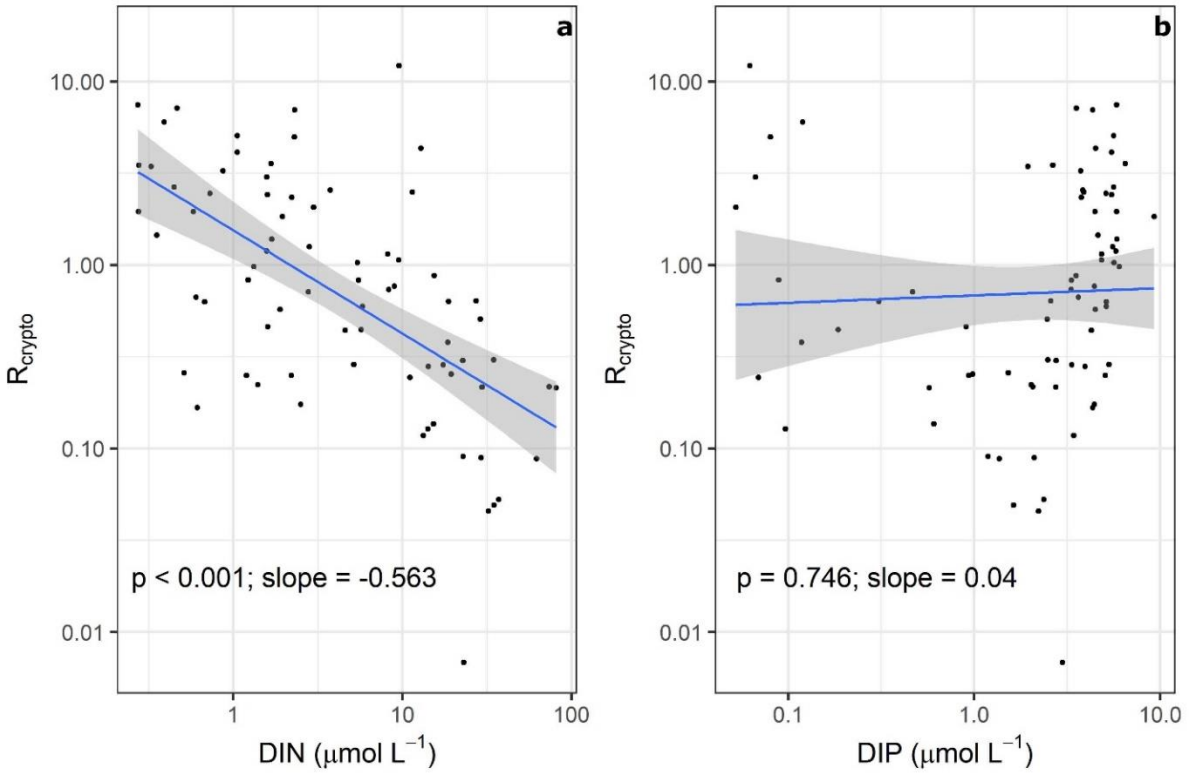

Fig. S1. Scatterplot showing the relationship between nutrient concentrations and R_{crypto} (ratio between *P. prolonga* to *T. amphioxeia*) in Roskilde Fjord (DK). (**A)** Dissolved inorganic nitrogen (DIN). (**b)** Dissolved inorganic phosphorus (DIP). Blue line represents the linear model and the shaded gray area represents the standard error. P value (α = 0. 05) and slope are provided in the graphs. Variables were log-transformed prior to analysis.

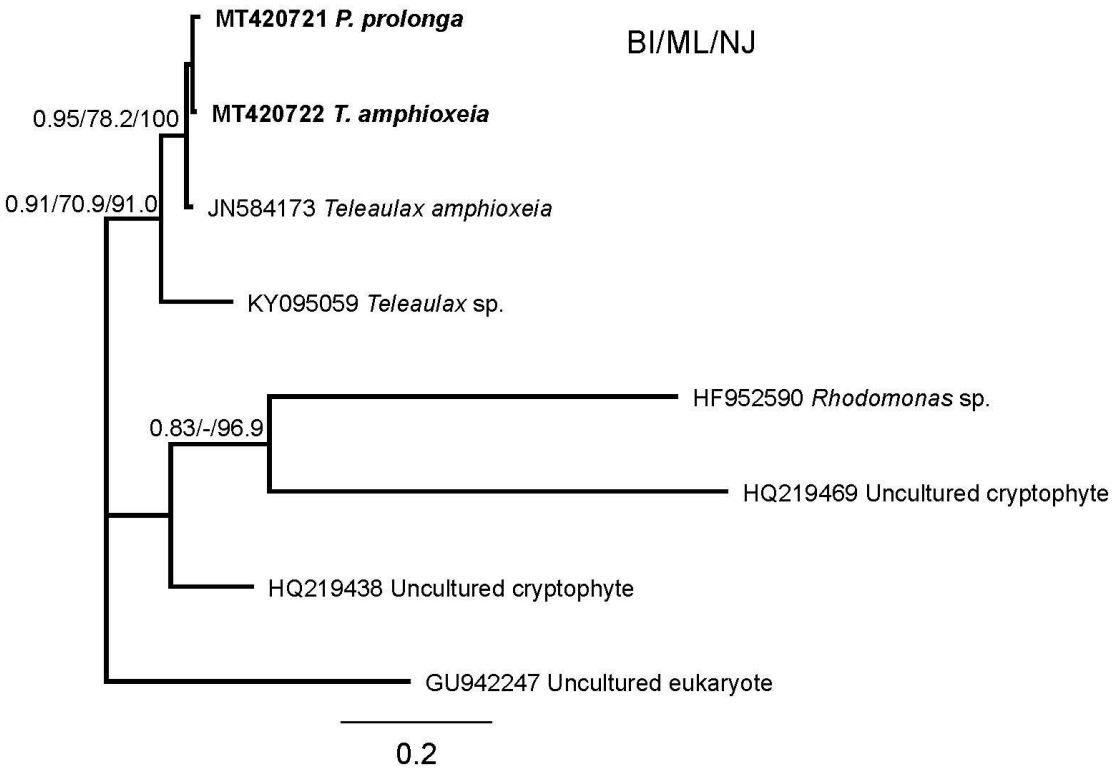

Fig. S2. Phylogenetic analysis of cryptophyte ITS sequences. The tree is based on Bayesian inference and includes newly sequenced *T. amphioxeia* and *P. prolonga* sequences in bold. Support values at nodes show posterior probability of Bayesian inference / bootstrap values of maximum likelihood / bootstrap values of neighbor-joining. Branches with support values below 70 are marked with (-). The scale bar corresponds to 20 nucleotide substitutions per 100 nucleotide positions.

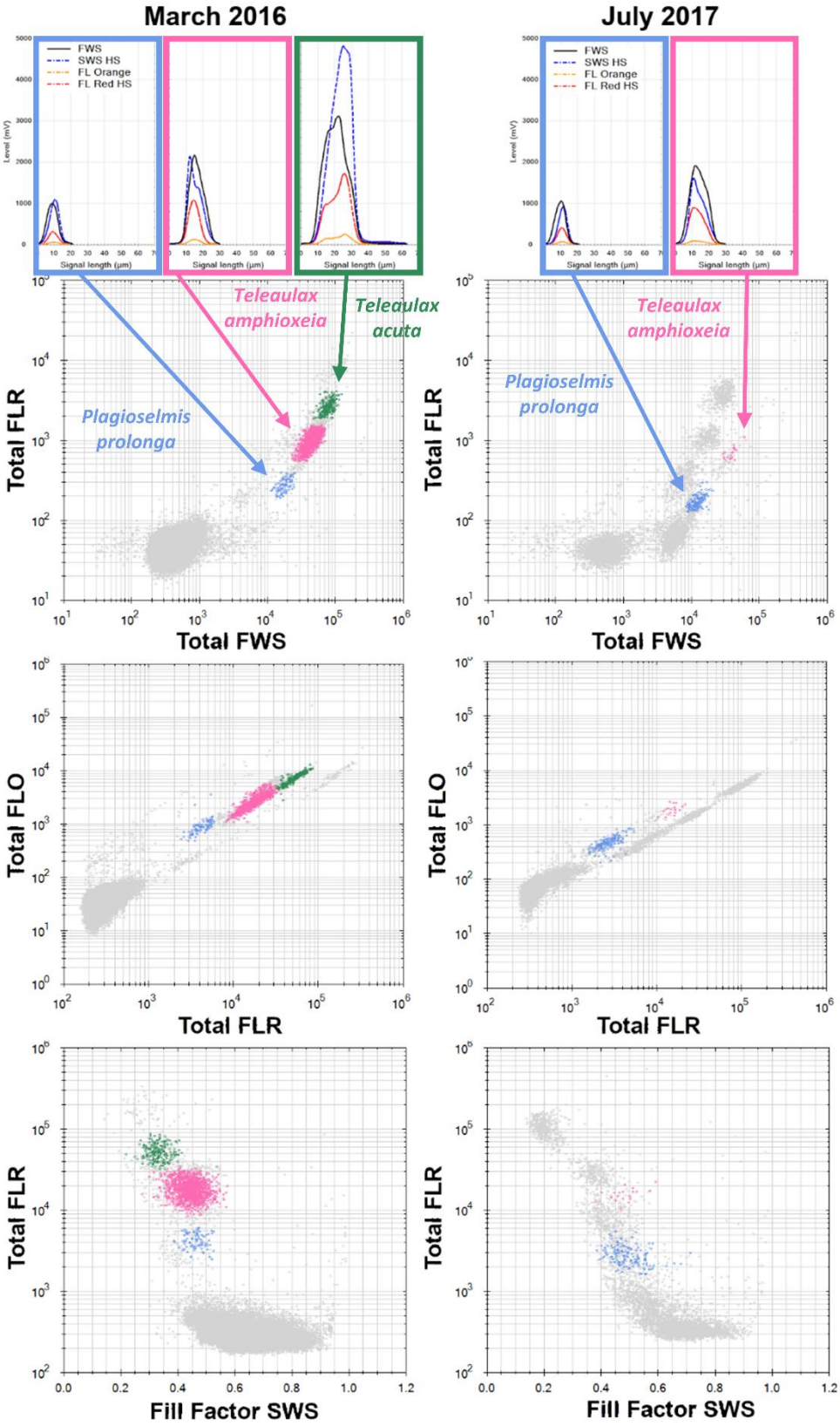

Fig S3. Example of Roskilde Fjord cryptophytes recorded by CytoSense. Pulse-shape optical profiles of representative cells and cytograms showing *P. prolonga* (light blue), *T. amphioxeia* (pink) and *T. acuta* (dark green, not discussed in this paper) clusters. Panels represent the phytoplankton communities in two contrasting seasons during the study period: March 2016 during a spring bloom (left panels), and July 2017, a period with low cryptophyte biomass in Roskilde Fjord (right panels).

Table S1. Summary of morphological differences between *T. amphioxeia* and the *P. prolonga* stage.

	T. amphioxeia	***P. prolonga stage***
Cell size	8-13 µm long, 3-6µm wide	6-8µm long, 3-5µm wide
Flagella	Ventral flagellum longer than the dorsal flagellum	Ventral flagellum shorter than the dorsal flagellum
Periplast	Sheet like	Hexagonal plates
Mid-ventral band	Short, curved, passing in oblique direction from the antapex; ca. 2.5µm in length	Prominent mid-ventral band extending from the antapical end of the furrow to the cell antapex; ca 4 µm in length

Table S2. Primer sequences used in PCR reactions.

Name	**Sequence 5' – 3'**	**Reference**
LSUR2	TCGGCAGGTGAGTTGTTAC	(*52*)
ITS1	TCCGTAGGTGAACCTGCGG	(*53*)
ITS4	TCCTCCGCTTATTGATATGC	(*53*)
SR4	AGGGCAAGTCTGGTGCCAG	(*54*)
SR6	GTCAGAGGTGAAATTCTTGG	(*54*)
SR7	TCCTTGGGCAAATGCTTTCGC	(*54*)
SR9p	AACTAAGAACRGCCATGCAC	(*54*)
SSUF (1F)	AACCTGGTTGATCCTGCCAGT	(*55*)
SSUR (1528R)	TGATCCTTCTGCAGGTTCACCTAC	(*55*)

REFERENCES AND NOTES

1. F. Cerino, A. Zingone, A survey of cryptomonad diversity and seasonality at a coastal Mediterranean site. *Eur. J. Phycol.* **41**, 363–378 (2006).

2. D. E. Gustafson, D. K. Stoecker, M. D. Johnson, W. F. Van Heukelem, K. Sneider, Cryptophyte algae are robbed of their organelles by the marine ciliate *Mesodinium rubrum*. *Nature* **405**, 1049–1052 (2000).

3. P. J. Hansen, M. Moldrup, W. Tarangkoon, L. Garcia-Cuetos, Ø. Moestrup, Direct evidence for symbiont sequestration in the marine red tide ciliate *Mesodinium rubrum*. *Aquat. Microb. Ecol.* **66**, 63–75 (2012).

4. K. Koike, K. Takishita, Anucleated cryptophyte vestiges in the gonyaulacalean dinoflagellates *Amylax buxus* and *Amylax triacantha* (Dinophyceae). *Phycol. Res.* **56**, 301–311 (2008).

5. M. G. Park, M. Kim, M. Kang, A dinoflagellate *Amylax triacantha* with plastids of the cryptophyte origin: phylogeny, feeding mechanism, and growth and grazing responses. *J. Eukaryot. Microbiol.* **60**, 363–376 (2013).

6. P. J. Hansen, L. T. Nielsen, M. Johnson, T. Berge, K. J. Flynn, Acquired phototrophy in *Mesodinium* and *Dinophysis* - A review of cellular organization, prey selectivity, nutrient uptake and bioenergetics. *Harmful Algae* **28**, 126–139 (2013).

7. E. Peltomaa, M. D. Johnson, *Mesodinium rubrum* exhibits genus-level but not species-level cryptophyte prey selection. *Aquat. Microb. Ecol.* **78**, 147–159 (2017).

8. P. Rial, A. Laza-Martinez, B. Reguera, N. Raho, F. Rodriguez, Origin of cryptophyte plastids in *Dinophysis* from Galician waters: results from field and culture experiments. *Aquat. Microb. Ecol.* **76**, 163–174 (2015).

9. B. L. Clay, P. Kugrens, R. E. Lee, A revised classification of Cryptophyta. *Bot. J. Linn. Soc.* **131**, 131–151 (1999).

10. K. Hoef-Emden, B. Marin, M. Melkonian, Nuclear and nucleomorph SSU rDNA phylogeny in the Cryptophyta and the evolution of cryptophyte diversity. *J. Mol. Evol.* **55**, 161–179 (2002).

11. K. Hoef-Emden, Molecular phylogeny of phycocyanin-containing cryptophytes: Evolution of biliproteins and geographical distribution. *J. Phycol.* **44**, 985–993 (2008).

12. D. R. A. Hill, R. Wetherbee, *Proteomonas sulcata* gen. et sp. nov. (Cryptophyceae), a cryptomonad with two morphologically distinct and alternating forms. *Phycologia* **25**, 521–543 (1986).

13. A. Houdan, C. Billard, D. Marie, F. Not, A. G. Sáez, J. R. Young, I. Probert, Holococcolithophore-heterococcolithophore (Haptophyta) life cycles: Flow cytometric analysis of relative ploidy levels. *Syst. Biodivers.* **1**, 453–465 (2004).

14. K. Hoef-Emden, M. Melkonian, Revision of the genus *Cryptomonas* (Cryptophyceae): a combination of molecular phylogeny and morphology provides insights into a long-hidden dimorphism. *Protist* **154**, 371–409 (2003).

15. M. Majaneva, I. Remonen, J.-M. Rintala, I. Belevich, A. Kremp, O. Setälä, E. Jokitalo, J. Blomster, *Rhinomonas nottbecki* n. sp. (Cryptomonadales) and molecular phylogeny of the family Pyrenomonadaceae. *J. Eukaryot. Microbiol.* **61**, 480–492 (2014).

16. A. Laza-Martinez, J. Arluzea, I. Miguel, E. Orive, Morphological and molecular characterization of *Teleaulax gracilis* sp. nov. and *T. minuta* sp. nov. (Cryptophyceae). *Phycologia* **51**, 649–661 (2012).

17. R. W. Butcher, An introductory account of the smaller algae of British coastal waters. Part IV: Cryptophyceae, in *Fishery Investigations, Series IV* (Her Majesty's Stationery Office, 1967), pp. 1–54.

18. N. J. Turland et al., *International Code of Nomenclature for algae, fungi, and plants (Shenzhen Code) adopted by the Nineteenth International Botanical Congress Shenzhen, China, July 2017* (Koeltz Botanical Books, Glashütten, 2018).

19. M.-J. Chrétiennot-Dinet, *Chlorarachnophycées, Chlorophycées, Chrysophycées, Cryptophycées, Euglénophycées, Eustigmatophycées, Prasinophycées, Prymnesiophycées, Rhodophycées et Tribophycées* (Atlas du phytoplancton marin, Éditions du CNRS, 1990) vol. 3.

20. G. Novarino, I. A. N. Lucas, S. Morrall, Observations on the genus *Plagioselmis* (Cryptophyceae). *Cryptogam. Algol.* **15**, 87–107 (1994).

21. D. R. A. Hill, A revised circumscription of *Cryptomonas* (Cryptophyceae) based on examination of Australian strains. *Phycologia* **30**, 170–188 (1991).

22. N. Daugbjerg, A. Norlin, C. Lovejoy, *Baffinella frigidus* gen. et sp. nov. (Baffinellaceae fam. nov., Cryptophyceae) from Baffin Bay: Morphology, pigment profile, phylogeny, and growth rate response to three abiotic factors. *J. Phycol.* **54**, 665–680 (2018).

23. F. Wawrik, Sexualität bei *Cryptomonas* sp. und *Chlorogonium maximum*. *Nova Hedwigia* **8**, 283–292 (1969).

24. F. Wawrik, Eisschluß- und Eisbruchvegetationen in den Teichen des nördlichen Waldviertels 1977/1978. *Arch. Protistenkd.* **122**, 247–266 (1979).

25. P. Kugrens, R. E. Lee, Ultrastructure of fertilization in a cryptomonad. *J. Phycol.* **24**, 385–393 (1988).

26. U. Goodenough, J. Heitman, Origins of eukaryotic sexual reproduction. *Cold Spring Harb. Perspect. Biol.* **6**, a016154 (2014).

27. D. Speijer, J. Lukes, M. Elias, Sex is a ubiquitous, ancient, and inherent attribute of eukaryotic life. *Proc. Natl. Acad. Sci. U.S.A.* **112**, 8827–8834 (2015).

28. M. Brandeis, New-age ideas about age-old sex: separating meiosis from mating could solve a century-old conundrum. *Biol. Rev.* **93**, 801–810 (2018).

29. Y. Ram, L. Hadany, Condition-dependent sex: who does it, when and why? *Philos. Trans. R. Soc. B* **371**, 1–8 (2016).

30. H. A. Thomsen, J. B. Østergaard, Circumstantial evidence of life history events in loricate choanoflagellates. *Eur. J. Protistol.* **58**, 26–34 (2017).

31. L. Peperzak, F. Colijn, E. G. Vrieling, W. W. C. Gieskes, J. C. H. Peeters, Observations of flagellates in colonies of *Phaeocystis globosa* (Prymnesiophyceae); a hypothesis for their position in the life cycle. *J. Plankton Res.* **22**, 2181–2203 (2000).

32. M. Valero, S. Richerd, V. Perrot, C. Destombe, Evolution of alternation of haploid and diploid phases in life cycles. *Trends Ecol. Evol.* **7**, 25–29 (1992).

33. M.-H. Nöel, M. Kawachi, I. Inouye, Induced Dimorphic Life Cycle of a Coccolithophorid, *Calyptrosphaera sphaeroidea* (Prymnesiophyceae, Haptophyta). *J. Phycol.* **40**, 112–129 (2004).

34. L. Haraguchi, H. H. Jakobsen, N. Lundholm, J. Carstensen, Phytoplankton community dynamic: A driver for ciliate trophic strategies. *Front. Mar. Sci.* **5**, 1–16 (2018).

35. A. J. Lewitus, D. A. Caron, Relative effects of nitrogen or phosphorus depletion and light intensity on the pigmentation, chemical composition, and volume of *Pyrenomonas salina* (Cryptophyceae). *Mar. Ecol. Prog. Ser.* **61**, 171–181 (1990).

36. D. R. A. Hill, *Teleaulax amphioxeia* Conrad (Hill), comb. nov. (Cryptophyceae). Baltic Sea Identification Sheet No. 13. *Ann. Bot. Fennici.*, 175–176 (1992).

37. L. Spear-Bernstein, K. R. Miller, Unique location of the phycobiliprotein light-harvesting pigment in the Cryptophyceae. *J. Phycol.* **25**, 412–419 (1989).

38. B. Walter, J. Peters, J. E. E. van Beusekom, The effect of constant darkness and short light periods on the survival and physiological fitness of two phytoplankton species and their growth potential after re-illumination. *Aquat. Ecol.* **51**, 591–603 (2017).

39. K. Grasshof, *Methods of Seawater Analysis* (Verlag Chemie, 1976).

40. J. Carstensen, in *Application of Threshold Concepts in Natural Resource Decision Making*, G. R. Guntenspergen, Ed. (Springer, 2014), pp. 255–272.

41. A. R. Loeblich III, V. E. Smith, Chloroplast pigments of the marine dinoflagellate *Gyrodinium resplendens*. *Lipids* **3**, 5–13 (1968).

42. M. L. Richlen, P. H. Barber, A technique for the rapid extraction of microalgal DNA from single live and preserved cells. *Mol. Ecol. Notes* **5**, 688–691 (2005).

43. G. Landan, D. Graur, Local reliability measures from sets of co-optimal multiple sequence alignments. *Pac. Symp. Biocomput.* **13**, 15–24 (2008).

44. I. Sela, H. Ashkenazy, K. Katoh, T. Pupko, GUIDANCE2: accurate detection of unreliable alignment regions accounting for the uncertainty of multiple parameters. *Nucleic Acids Res.* **43**, W7–W14 (2015).

45. S. Guindon, J.-F. Dufayard, V. Lefort, M. Anisimova, W. Hordijk, O. Gascuel, New algorithms and methods to estimate maximum-likelihood phylogenies: assessing the performance of PhyML 3.0. *Syst. Biol.* **59**, 307–321 (2010).

46. V. Lefort, J. E. Longueville, O. Gascuel, SMS: Smart Model Selection in PhyML. *Mol. Biol. Evol.* **34**, 2422–2424 (2017).

47. J. P. Huelsenbeck, F. Ronquist, MRBAYES: Bayesian inference of phylogenetic trees. *Bioinformatics* **17**, 754–755 (2001).

48. A. Nabbi, K. Riabowol, Rapid isolation of nuclei from cells in vitro. *Cold Spring Harb Protoc* **2015**, 769–772 (2015).

49. D. Marie, F. Partensky, S. Jacquet, D. Vaulot, Enumeration and cell cycle analysis of natural populations of marine picoplankton by flow cytometry using the nucleic acid stain SYBR Green I. *Appl. Environ. Microbiol.* **63**, 186–193 (1997).

50. G. B. Dubelaar, P. J. Geerders, R. R. Jonker, High frequency monitoring reveals phytoplankton dynamics. *J. Environ. Monit.* **6**, 946–952 (2004).

51. M. Thyssen, S. Alvain, A. Lefèbvre, D. Dessailly, M. Rijkeboer, N. Guiselin, V. Creach, L.-F. Artigas, High-resolution analysis of a North Sea phytoplankton community structure based on in situ flow cytometry observations and potential implication for remote sensing. *Biogeosciences* **12**, 4051–4066 (2015).

52. Y. Takano, T. Horiguchi, Surface ultrastructure and molecular phylogenetics of four unarmored heterotrophic dinoflagellates, including the type species of the genus *Gyrodinium* (Dinophyceae). *Phycol. Res.* **52**, 107–116 (2004).

53. T. J. White, T. Bruns, S. Lee, J. Taylor, in *PCR Protocols: A Guide to Methods and Applications*, M. A. Innis, J. J. Gelfand, J. J. Sninsky, T. J. White, Eds. (Academic Press, 1990), pp. 315–322.

54. A. Yamaguchi, T. Horiguchi, Molecular phylogenetic study of the heterotrophic dinoflagellate genus *Protoperidinium* (Dinophyceae) inferred from small subunit rRNA gene sequences. *Phycol. Res.* **53**, 30–42 (2005).

55. L. Medlin, H. J. Elwood, S. Stickel, M. L. Sogin, The characterization of enzymatically amplified eukaryotic 16S-like rRNA-coding regions. *Gene* **71**, 491–499 (1988).